Inverse Scattering Via Virtual Experiments and Contrast Source Regularization

Loreto Di Donato, Martina Teresa Bevacqua, Lorenzo Crocco, *Senior Member, IEEE*, and Tommaso Isernia, *Member, IEEE*

***Abstract*—In microwave imaging, the linearity of the relationship between the incident and the scattered field offers the possibility of *a posteriori* recombining the performed scattering experiments and then to cast the underlying inverse problem with respect to the resulting, *virtual*, ones. The interest of such a circumstance is that properly designed virtual experiments can enforce particular and convenient conditions. In this paper, we present an application of this paradigm to the popular contrast source inversion (CSI) method. In particular, we first design a set of virtual experiments capable to induce contrast sources exhibiting circular symmetries (with respect to some *pivot* points). Then, we devise an original and effective regularized CSI scheme, in which a penalty term is added to the usual cost functional, in order to account for the symmetry of the auxiliary unknowns. Notably, the approach does not require any *a priori* assumption on the unknown contrast, as it relies on the particular nature of the virtual contrast sources. Results with single frequency Fresnel experimental data are given to assess the capabilities of the proposed approach.**

***Index Terms*—Contrast source inversion (CSI), electromagnetic inverse scattering problems, linear sampling method (LSM), microwave imaging, virtual scattering experiments.**

I. Introduction

INVERSE scattering problems are relevant to several applications of electromagnetic waves, such as nondestructive testing, subsurface prospecting, and biomedical imaging. However, to pursue the characterization of an unknown obstacle, a nonlinear and ill-posed inverse problem has to be faced [1].

In this respect, a class of solution approaches that is broadly adopted is the one of modified gradient (MG) methods [2]–[6], in which the inverse problem is cast as the minimization of a cost function. Such a function depends on both the unknown contrast (that encodes the obstacle properties) and an auxiliary unknown, which can be the field in the imaging domain [2], [4] or the contrast source therein induced [3], [5], [6]. These methods do not require any approximation (but for the obvious discretization), nor an explicit solution of the forward problem at each step. Moreover, they allow to deal with a manageable degree of nonlinearity, thanks to the introduction of the auxiliary unknown.

However, similar to other nonlinear inversion schemes, MG methods are based on local iterative optimization, so that they are prone to the occurrence of false solutions [4], [7]. Therefore, ongoing efforts have been devoted to devise strategies able to defeat the ill-posedness of the problem, as well as the occurrence of false solutions. For instance, widely adopted and effective schemes are the Tikhonov regularization [8], the multiplicative regularization (MR) [9], the total variation minimization scheme [10], or the projection method, in which the unknowns are represented by the coefficients of a suitable representation basis [4], [5], [11]–[13]. Notably, all these schemes enforce a regularization of the ill posed inverse problem, and try to defeat its nonlinearity by imposing constraints on the contrast function. This implies that the choice of the most suitable one depends on the expected contrast properties (for instance, smoothness and piece-wise constant behavior).

With respect to the canonical two-dimensional (2-D) scalar problem in free space, in this paper, we explore a novel and different strategy, in which the nonlinearity of the problem is tackled by acting on the auxiliary unknown rather than on the contrast. The proposed strategy relies on an emerging paradigm for microwave imaging, which consists in taking advantage of experiments that are designed in such a way to enforce some specific behavior of the field or of the contrast source which generate this field [14]–[18]. Notably, these experiments are implemented in a synthetic way, that is, without performing additional measurements, but simply processing the available ones. In particular, we explore the possibilities offered by this simple and powerful concept in the framework of the popular contrast source inversion (CSI) scheme [3].

To this end, we consider (and show how to design) a set of virtual experiments capable to induce contrast sources that are circularly symmetric (in terms of spatial distribution of these sources, not of their shape or topology) with respect to some properly chosen points within the imaging domain. Then, we cast the CSI scheme for the designed virtual experiments and introduce an additive penalty term that improves the global optimization process by enforcing the expected contrast source properties.

Manuscript received March 05, 2014; revised October 24, 2014; accepted January 04, 2015. Date of publication January 14, 2015; date of current version April 03, 2015.

L. Di Donato is with DIEEI, Department of Electrical, Electronics, and Computer Science, University of Catania, 95126 Catania, Italy (e-mail: loreto.didonato@dieei.unict.it).

M. T. Bevacqua is with DIIES, Department of Information Engineering, Infrastructures and Sustainable Energy, Università Mediterranea di Reggio Calabria, 89124 Reggio di Calabria, Italy (e-mail: martina.bevacqua@unirc.it).

L. Crocco is with CNR-IREA, National Research Council of Italy–Institute for Electromagnetic Sensing of the Environment, 80124 Naples, Italy (e-mail: crocco.l@irea.cnr.it).

T. Isernia is with DIIES, Department of Information Engineering, Infrastructures and Sustainable Energy, Università Mediterranea di Reggio Calabria, 89124 Reggio di Calabria, Italy, and also with CNR-IREA, National Research Council of Italy–Institute for Electromagnetic Sensing of the Environment, 80124 Napoli, Italy (e-mail: tommaso.isernia@unirc.it).

Color versions of one or more of the figures in this paper are available online at http://ieeexplore.ieee.org.

Digital Object Identifier 10.1109/TAP.2015.2392124

0018-926X © 2015 IEEE. Personal use is permitted, but republication/redistribution requires IEEE permission.
See http://www.ieee.org/publications_standards/publications/rights/index.html for more information.
Authorized licensed use limited to: UNIVERSIDADE FEDERAL DE MINAS GERAIS. Downloaded on May 28,2024 at 12:59:07 UTC from IEEE Xplore. Restrictions apply.

It is worth noting that, different from the schemes recalled above, the one presented here does not rely on *a priori* information on the contrast function. Rather, it may be related to the subspace optimization method (SOM) [6], as also SOM pursues the inversion stability by acting on the auxiliary unknown. However, the two methods are deeply different. Moreover, as in SOM-MR scheme [19], the proposed approach can be used in conjunction with regularization schemes acting on the contrast. However, such an issue is outside of the scope of the present paper, which is focused on the introduction, discussion, and experimental validation of the proposed strategy and procedures.

The paper is organized as follows. In Section II, we formulate the inverse scattering problem and recall the CSI method. In Section III, we outline the simple concepts underlying the virtual experiments' framework. In Section IV, we give criteria and tools to design a set of virtual experiments capable of inducing circularly symmetric contrast sources. In Section V, we introduce the new CSI approach using a contrast source regularization (or conditioning). In Section VI, we first assess the performance of the approach against some of the Fresnel experimental datasets [20], [21], and then present some numerical simulations to address, some particularly, interesting cases. Throughout the paper, the time harmonic factor $\exp(\jmath\omega t)$ is omitted.

II. Statement of the Problem and the CSI Inversion Scheme

Let $D \subseteq \Re^2$ denote the investigation domain that contains the cross-section Σ of one or more dielectric nonmagnetic scatterers, whose properties are related to those of the homogeneous host medium through the contrast function

$$\chi(\underline{r}) = \epsilon_s(\underline{r})/\epsilon_b - 1 \tag{1}$$

wherein $\underline{r} = (x, y)$, and ϵ_s and ϵ_b are the relative (possibly complex) permittivity of the scatterer and the background medium, respectively.

By assuming the TM polarization for the electric field, the equations governing the scattering phenomenon for the geometry at hand can be expressed in an integral form by means of the contrast source formulation as follows:

$$\begin{aligned} E_s(\underline{r}_m, \underline{r}_t) &= \int_D G(\underline{r}_m, \underline{r}')W(\underline{r}', \underline{r}_t)d\underline{r}' \\ &= \mathbb{G}_R[W], \quad \underline{r}_m \in \Gamma_R \end{aligned} \tag{2}$$

$$\begin{aligned} W(\underline{r}, \underline{r}_t) - \chi(\underline{r})E_i(\underline{r}, \underline{r}_t) &= \chi(\underline{r}) \int_D G(\underline{r}, \underline{r}')W(\underline{r}', \underline{r}_t)d\underline{r}' \\ &= \chi(\underline{r})\mathbb{G}_D[W], \quad \underline{r} \in D \end{aligned} \tag{3}$$

wherein E_i is the incident field radiated by a source positioned in $\underline{r}_t = (R, \theta) \in \Gamma_T$, with Γ_T being a curve external to D, E_s is the corresponding scattered field as measured at $\underline{r}_m = (R, \phi) \in \Gamma_R$, with Γ_R being a curve external to D, W is the contrast source induced in D by E_i and G is the Green's function, which, for the 2-D case at hand, reads $G(\underline{r}, \underline{r}') = \frac{-j}{4}k_b^2 H_0^{(2)}(k_b|\underline{r} - \underline{r}'|)$, k_b being the wave-number in the host medium and $H_0^{(2)}$ being the zero-order second kind Hankel function. The Green's function is the kernel of the radiation operators $\mathbb{G}_R[\cdot] : L^2(D) \to L^2(\Gamma_R)$ and $\mathbb{G}_D[\cdot] : L^2(D) \to L^2(D)$ that relate the contrast sources in D to the field they radiate on Γ_R and in D, respectively.

The inverse scattering problem aims at retrieving the unknown contrast $\chi \; \forall \; r \in D$ from the scattered fields E_s measured for several receiving positions $\underline{r}_m$, and for a set of known incident fields E_i radiated by several source positions $\underline{r}_t \in \Gamma_T$. As well known, such a problem is nonlinear and ill-posed. The former circumstance descends from the dependance of the contrast source W on the unknown contrast function χ, while the latter from the compactness of the radiation operator $\mathbb{G}_R$ [22], [23].

In particular, due to ill-posedness, only a finite number of independent experiments (and measurements) are available and hence only a limited number of independent parameters can be recovered from scattered field data [22], [24], [25]. Accordingly, we will consider from now on a finite number of scattering experiments. In so doing, care has to be taken in choosing the positions $R_t^1, \ldots, R_t^N$ of the N transmitting probes on Γ_T and those of the receiving ones, $R_m^1, \ldots, R_m^M$ on Γ_R, in such a way to collect all the available information in a nonredundant fashion. This can be efficiently done by adopting the measurement strategies proposed in [22], wherein a Nyquist criterion is essentially suggested for the case at hand.

The CSI scheme tackles the problem looking for both the unknown contrast χ and the auxiliary unknown W. In particular, the problem's solution is defined as the global minimum of the cost functional

$$\begin{aligned} \Phi_{CS}\left(\chi, W^{(1)}, \ldots, W^{(N)}\right) &= \sum_{v=1}^{N} n_R^v \left\| E_s^{(v)} - \mathbb{G}_R\left[W^{(v)}\right] \right\|_{\Gamma_T}^2 \\ &+ \sum_{v=1}^{N} n_D^v \left\| W^{(v)} - \chi E_i^{(v)} - \chi\mathbb{G}_D\left[W^{(v)}\right] \right\|_D^2 \end{aligned} \tag{4}$$

wherein $\|\cdot\|$ denotes the usual L^2 norm and n_R^v and n_D^v are normalization coefficients.

Due to the large number of unknown parameters, the minimization of the cost functional (4) has to be tackled by means of local optimization. Hence, due to nonlinearity, the procedure provides the correct result only for an initial estimate that lies in the attraction basin of the solution. As this is not always the case (and since it is not possible to foresee in general whether or not the initial guess is "good"), regularization schemes are introduced to overcome this problem. As recalled in the introduction, typically (but for SOM [6]) this consists in enforcing some assumed or expected properties of the unknown contrast. A second approach acting on W (rather than on χ) is presented in the following.

III. Virtual Experiments as a Way to Re-Weight the Measured Information

Although the problem's formulation given in the previous Section is the typical and mostly used one, an interesting circumstance descends from the inherent linearity of the scattering

Authorized licensed use limited to: UNIVERSIDADE FEDERAL DE MINAS GERAIS. Downloaded on May 28,2024 at 12:59:07 UTC from IEEE Xplore. Restrictions apply.

phenomenon for a fixed contrast function. According to this property, a superposition of the incident fields gives rise to a scattered field, which is nothing but the same superposition of the corresponding scattered fields.

Hence, if we consider a superposition of the incident fields $E_i(\underline{r}, \underline{R}_t^n)$, $n = 1, \ldots, N$, radiated by the probes positioned in $R_t^1, \ldots, R_t^N$

$$\mathcal{E}_i(\underline{r}) = \sum_{n=1}^{N} \alpha_n E_i(\underline{r}, \underline{R}_t^n) \tag{5}$$

such an incident field will give rise to the contrast source

$$\mathcal{W}(\underline{r}) = \sum_{n=1}^{N} \alpha_n W(\underline{r}, \underline{R}_t^n) \tag{6}$$

and finally, this latter will produce the scattered field

$$\mathcal{E}_s(\underline{R}_m^i) = \sum_{n=1}^{N} \alpha_n E_s(\underline{R}_m^i, \underline{R}_t^n), \quad i = 1, \ldots, M. \tag{7}$$

Accordingly, performing several re-arrangements of the original experiments, it is possible to build a set of new experiments. We will refer to these latter as *virtual* experiments, to remark that no further experimental measurement is required, as they are derived from *a posteriori* software procedures.

Obviously, virtual experiments are just a different way to consider, or saying it better, to "re-weight" the originally collected information, so that the above-mentioned issues on the finite amount of independent information available to solve the inverse problem still hold true.[1]

Nevertheless, as long as they are properly designed, one can tackle the original problem in terms of virtual experiments, rather than reasoning in terms of original ones. In [14], [16] and [17], [18] such a concept has been used to devise new approximations for the internal fields and the contrast sources, respectively, and exploited to cast new approximated inversion methods capable of working well beyond traditional linear approximations. In [15], the field approximation used in [14] was instead exploited as a convenient starting guess for a field-based MG inversion scheme. Different from these contributions, in the following, we apply this concept to the CSI framework, by casting the scheme with respect to virtual experiments capable of enforcing contrast sources having a circular symmetric structure and introducing a regularization term that accounts for this circumstance. In the Section IV, we show how to design such a kind of experiments.

IV. Synthesizing Circularly Symmetric Contrast Sources Via Virtual Experiments

To design a set of virtual experiments, the scattered fields collected in the original experiments are the only available data, so that one has to act on them to pursue the design goal.

Accordingly, to achieve the specific set of virtual experiments we are aiming to, we enforce a circular symmetry of the scattering phenomenon around given points. That is, we pursue the design of experiments such that each virtual scattered field exhibits (within some required accuracy) a circular symmetry around some *pivot* point.

Such a goal can be accomplished by requiring that the virtual scattered fields $\mathcal{E}_s$ fulfill the following equation:

$$\sum_{n=1}^{N} \alpha_n^p E_s\left(\underline{R}_m^i, \underline{R}_t^n\right) = \sqrt{\frac{2}{\pi k_b |\underline{R}_m^i - r_p|}} e^{-\jmath k_b |\underline{R}_m^i - \underline{r}_p|} \tag{8}$$

where $\underline{r}_p$ is the considered pivot point, $i = 1, \ldots, M$ and $\boldsymbol{\alpha}_\mathbf{p} = \{\alpha_1^p, \ldots, \alpha_N^p\}$ identify the combination coefficients required to implement the virtual scattering experiments that give rise to the sought circular symmetry around $\underline{r}_p$. In fact, assuming that one is able to determine these coefficients, by virtue of (5)–(7), they also define the incident field that gives rise to the contrast source radiating such a scattered field.

Interestingly, (8) is nothing but the discretized version of the well-known "far field" equation, i.e., the basic (linear) equation underlying the linear sampling method (LSM) [26], with $\underline{r}_p$ playing the role of the *sampling* point. Accordingly, the problem cast in (8) is ill-conditioned and has to be solved through some regularization strategy. We refer the reader to [27], [28] for detail on the implementation of the regularized solution of (8).

Here, we adopt the Tikhonov regularization, which has also an effect on the synthesized contrast source. In fact, the minimum energy requirement (on the primary sources) enforced by the Tikhonov regularization corresponds to minimize the nonradiating component of the contrast sources [29]. As a consequence, as long as (8) is fulfilled (in a regularized sense), the resulting virtual contrast source will exhibit an essentially circularly symmetric structure with respect to the pivot point at hand.

Taking the above circumstance into account, in the following we present a new regularization scheme for CSI, in which the scattering problem is recast into a set of virtual experiments (rather than the original multiview multistatic ones) and circularly symmetric contrast sources are looked for. Notably, such an assumption entails that circularly symmetric nonradiating sources are also taken into account in the model, while angularly varying (radiating and nonradiating) contrast sources are instead neglected, as they are expected to be small.

V. New Regularized CSI Strategy

Let us assume that (8) has been applied to the whole imaging domain D. Then, let $r_p^1, \ldots, r_p^P$ be a set of P pivot points for which the equation has been solved (in a regularized sense) and denote with $\boldsymbol{\alpha}_\mathbf{1}, \ldots, \boldsymbol{\alpha}_\mathbf{P}$ the sets of corresponding coefficients.

Now, it is possible to recast the original problem given in (3) and (2), in terms of the obtained virtual scattering experiments, in which a circular symmetry of the contrast sources around the selected pivot points is expected.

To this end, we define the set of virtual incident fields

$$\mathcal{E}_i^{(p)}(\underline{r}) = \sum_{n=1}^{N} \alpha_n^p E_i(\underline{r}, \underline{R}_t^n), \quad p = 1, \ldots, P \tag{9}$$

[1] Actually, care has to be taken in generating virtual experiments in order to avoid loss of significant information, as we are going to show in Section V-A.

Authorized licensed use limited to: UNIVERSIDADE FEDERAL DE MINAS GERAIS. Downloaded on May 28,2024 at 12:59:07 UTC from IEEE Xplore. Restrictions apply.

which, by construction, give rise to scattered fields that approximate cylindrical waves emanating from the generic r_p. These latter can be expressed as

$$\mathcal{E}_s^{(p)}\left(\underline{R}_m^i\right) = \sum_{n=1}^{N} \alpha_n^p E_s\left(\underline{R}_m^i, \underline{R}_t^n\right) \tag{10}$$

with $p = 1, \ldots, P$ and $i = 1, \ldots, M$.

With respect to the virtual experiments devised above, we now consider the CSI scheme (4), as recast for the recombined data and equipped with an additional regularizing term that account for the peculiar structure of the enforced virtual contrast sources, which reads

$$\begin{aligned}\Phi_{VCS}\left(\chi, \mathcal{W}^{(1)}, \ldots, \mathcal{W}^{(P)}\right) &= \sum_{p=1}^{P} \frac{\left\|\mathcal{E}_s^{(p)} - \mathbb{G}_R\left[\mathcal{W}^{(p)}\right]\right\|_{\Gamma_T}^2}{\left\|\mathcal{E}_s^{(p)}\right\|_{\Gamma_T}^2} \\ &+ \sum_{p=1}^{P} \frac{\left\|\mathcal{W}^{(p)} - \chi\mathcal{E}_i^{(p)} - \chi\mathbb{G}_D\left[\mathcal{W}^{(p)}\right]\right\|_D^2}{\left\|\mathcal{E}_i^{(p)}\right\|_D^2} \\ &+ \Phi\left(\mathcal{W}^{(1)}, \ldots, \mathcal{W}^{(P)}\right)\end{aligned} \tag{11}$$

wherein the fields are given by (9) and (10), and

$$\Phi = \sum_{p=1}^{P} \tau_p \left\|\frac{\partial \mathcal{W}^{(p)}}{\partial \phi_p}\right\|_D^2, \quad \underline{r} \in \Omega_p \tag{12}$$

where ϕ_p is the angular coordinate of a local polar reference system centered in $\underline{r}_p$ which spans the circular neighborhood Ω_p, and $\{\tau_p\}_1^P$ are nonnegative parameters controlling the relative weight of such a regularization term. Hence, (12) is a way to enforce the expected contrast sources' properties by minimizing the angular variation of each $\mathcal{W}^{(p)}$ around the pertaining pivot point $\underline{r}_p$.

Note that, different from the usual CSI scheme [3], the minimization of the cost function (11) is carried by simultaneously updating both the contrast and the contrast source, using the same scheme as in [4]. While we refer the reader to that work for the general structure of the optimization procedure, the implementation of the new regularization term in the framework of a gradient-projection optimization is detailed in the Appendix. As a further difference, note that the normalization term for the "state" equation is usually given by the norm of the product of the contrast times the incident field. Although this seems a natural choice, it has the drawback of changing, in an unpredictable way, the metric at each iteration of the minimization process. For this reason, we use as normalization factor just the norm of the (virtual) incident field.

A. On the Choice of $\underline{r}_p$, Ω_p, and τ_p

To set the parameters appearing in the inversion procedure (the pivot points $\underline{r}_p$, the weight τ_p, and radius of Ω_p), we take advantage of the fact that our design equation (8) also provides an estimate of the unknown targets' support. As a matter of fact, (8) is the equation adopted in LSM, wherein such an information is simply obtained by plotting the norm of the solution $\|\boldsymbol{\alpha}_\mathbf{p}\|$, over the imaging domain D, as this latter acts as an "indicator" of the scatterers' support.

In particular, we use the normalized indicator function as defined in [28]

$$\Upsilon = \frac{\log_{10}\|\boldsymbol{\alpha}_\mathbf{p}\| - \log_{10}\|\boldsymbol{\alpha}_\mathbf{p}\|_{\max}}{\min\left[\log_{10}\|\boldsymbol{\alpha}_\mathbf{p}\| - \log_{10}\|\boldsymbol{\alpha}_\mathbf{p}\|_{\max}\right]} \tag{13}$$

which continuously varies between 0 and 1 and assumes largest values in points belonging to the scatterers.

Let us first discuss the choice of the pivot points $\underline{r}_p$, noting that they are not meant as a sampling of the scatterer permittivity.[2] Rather, their choice has to ensure that the resulting virtual experiments are capable of enforcing the expected behavior of the contrast sources. Hence, pivot points whose corresponding (virtual) scattered fields more closely resemble cylindrical waves should be preferred. In fact, such a condition entails a better circularity of the contrast sources $\mathcal{W}$.

Accordingly, the choice of the pivot points is carried out following the simple rules which follow.

1) First of all, we choose the pivot points $\underline{r}_p$ among those that are understood to belong to the estimated support, as provided by Υ.
2) Then, as far as their number is concerned, we note that the number of independent scattering experiments depends on the dimensions of the scatterer [22], so that we choose a number of pivot points in the order of that deriving from the estimated dimensions of the scatterer (via Υ). Note that it is important to not underestimate the number of experiments, so to carry all of the information gathered by the original experiments in the virtual framework. Conversely, considering a larger number would "only" have a drawback in terms of computational burden.
3) Finally, as far as their location is concerned, the pivot points should be such that enforcing a circular contrast source is possible. Therefore, they should not be too close to the border of the scatterer (as estimated from Υ). Also, they should be preferably located in those parts of the region under test where Υ attains values close to 1, as these are the point where enforcing a circularly symmetric source is expected to be simpler [27], [29], [30].
   In doing so, one should also avoid to cancel any significant information carried by the original experiments. To this end, pivot points must be chosen not too close each others, as the information carried by virtual experiments of clustered pivots would be nearly the same. In practice, the available pivot points are evenly spaced within the estimated support. In [14], it has been shown that this is indeed the most effective strategy to build independent virtual experiments.

To select the suitable radius of the circular domain Ω_p, we recall that the contrast source must have the same support Σ as the scatterer [27], [30]. Hence, the maximum allowed value for

[2]This would be obviously impossible, being the permittivity distribution unknown.

Authorized licensed use limited to: UNIVERSIDADE FEDERAL DE MINAS GERAIS. Downloaded on May 28,2024 at 12:59:07 UTC from IEEE Xplore. Restrictions apply.

the radius of Ω_p will be ruled by the distance between $\underline{r}_p$ and the estimated boundary of the scatterer. Note this means that circular domain of different radius (and extent) will be adopted for the different pivot points, depending on the distance from the boundary. In particular, the closer the pivot point to the (estimated) borders of the scatter, the smaller the radius of the corresponding Ω_p.

Similar arguments can be exploited for the choice of τ_p. In particular, since the contrast source's support is constrained onto Σ, we expect that the induced current for $\underline{r}_p$ close to the estimated boundary will not show an exact circular symmetry (with respect to $\underline{r}_p$), [27], [30]. This physical observation corresponds to what is foreseen by LSM theory, according to which the energy of the solution $\|\boldsymbol{\alpha}_{\mathbf{p}}\|$ blows up when $\underline{r}_p$ approaches the boundary of the scatterer [31]. Accordingly, we can devise an automatic way to select τ_p by relying on the LSM indicator. In particular, we set τ_p equal to the value obtained by Υ in the relevant $\underline{r}_p$. Note this allows to set values of τ_p in the range [0,1].

VI. Assessing the Method

To assess the proposed approach, we have exploited the experimental data provided by the Institute Fresnel of Marseille, France, which is the subject of the Section VI-A. Moreover, as the LSM is known to get into troubles when dealing with not simply connected objects, we also analyze and discuss in Section VI-B the case of a ring-like target.

A. Assessing the Method Using Single Frequency Fresnel Data

As a first assessment, consideration of Fresnel data, which have been explicitly conceived to emulate 2-D scatterers, is in order. In particular, we have considered three different targets:

1) the $TwinDielTM$ target [20], which consists of two identical dielectric cylinders of radius 1.5 cm and relative permittivity 3 ± 0.3;
2) the $FoamDielIntTM$ target [21], which is a piece-wise inhomogeneous dielectric target made by two nested, non concentric, circular cylinders, a high contrast inner one ($\epsilon = 3 \pm 0.3$), and a low contrast outer one ($\epsilon = 1.45$);
3) the $FoamTwinDielTM$ target [21], in which a circular cylinder having the same dimensions and features of the high contrast core is placed in contact with the $FoamDielIntTM$ target.

Notably, unlike most of the results reported in the literature, see for instance [9], [32]–[35] and similarly to the remarkable exception [36], [18], we have obtained the reconstructions reported in the following by simply using single frequency data and without enforcing (through regularization) *a priori* information on the unknown contrast.

The complete description of the targets and the measurement setup can be found in [20], [21]. We just recall here that the experiments have been carried out under a partially aspect limited configuration, in which the illuminations completely surround the targets, but, for each illumination, the measurements are taken only on an angular sector of 240°, that is, excluding a 120° sector centered on the incidence direction. In particular, for the first test bed, $N = 36$ illumination directions and $M = 49$ measurements for each view are considered, for the second one $N = 72$ and $M = 61$, and for the third target $N = 18$ and $M = 241$. As the database provides the incident field only at the receiving locations, the incident fields inside the imaging domain have been estimated from these latter by means of the procedure outlined in [34].

In all cases, we have not enforced throughout the minimization any constraint on the admissible values of permittivity and conductivity (which must be respectively larger than 1 and positive, being the vacuum the background medium). Note that this is a significant difference with respect to several previous contributions, for instance [32] and [33].

To build the virtual experiments and cast the corresponding scattering equations for each target, we have first processed the data by solving the "design" equation (8) onto an arbitrary grid of points that samples the imaging domain D, which is a square of side ℓ_D. To this end, as in [27], we have replaced with zeros the "missing" entries in the data matrix (i.e., the field values at the measurement points that would lie on the 120° arc centered onto the illumination direction) and solved the resulting ill-conditioned matrix equation using Tikhonov regularization, in which the weighting parameter (the same for all the sampling points) has been fixed following the guidelines in [37]. In particular, the adopted parameter is equal to 2.5×10^{-3}, 5.6×10^{-5}, 8.8×10^{-4}, respectively.

Finally, we plot the indicator Υ (13) over D to obtain an estimate of the target's shape and chose the pivot points' locations according to the rules in Section V-A. With respect to the resulting virtual experiments, we run the minimization of the regularized cost functional (11) to obtain the reconstruction of the unknown contrast.

The results of the design step and the resulting reconstructions for the three considered Fresnel targets are shown in Fig. 1. As it can be noticed, even if no *a priori* information on the target's nature has been enforced and no regularization is enforced on the contrast function, the dielectric permittivity value is accurately (i.e., quantitatively) retrieved in all cases. Note that the reconstructions obtained, in the same conditions, with the basic version of CSI approach and without the term (12), do not converge to the actual solution, thus confirming the actual regularizing nature of the proposed procedure. It is also worth underlining that some of the selected pivot points do not belong to the actual support of the target, so that we can state that the proposed method is indeed robust with respect to uncertainties that may occur in their choice.

Table I summarizes the details of the inversion procedures carried out for the three considered datasets, i.e., the adopted frequency, the size of the imaging domain, the actual size of the data matrix processed in the design step and the radius of Ω_p (which changes for the innermost, inner and outermost pivot points) in terms of the background wavelength λ_b.

B. Assessment of Performances in Case of Nonsimply Connected Objects

In this section, we show how the method is robust to possible errors in the design step, by considering a target which is

Authorized licensed use limited to: UNIVERSIDADE FEDERAL DE MINAS GERAIS. Downloaded on May 28,2024 at 12:59:07 UTC from IEEE Xplore. Restrictions apply.

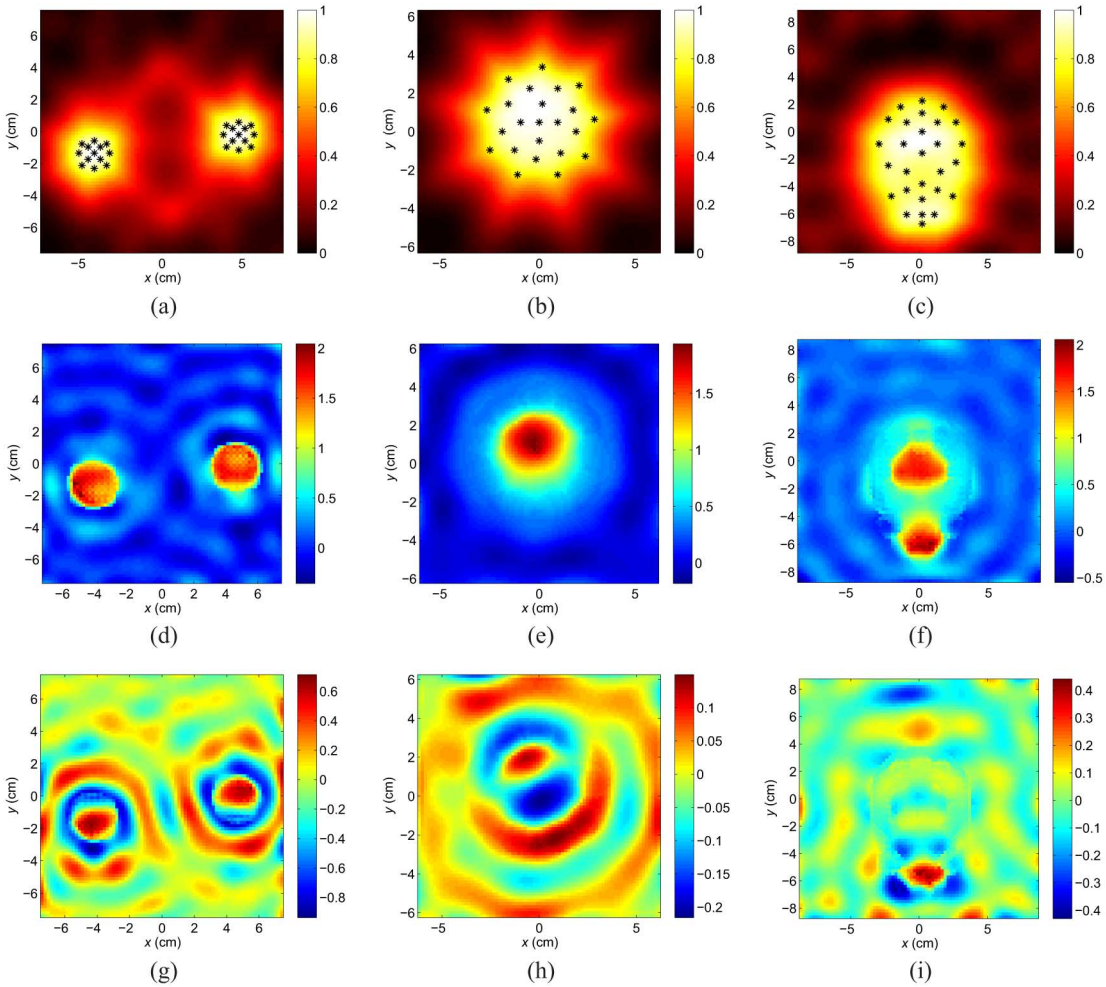

Fig. 1. Assessing the proposed method against Fresnel experimental data. Shape reconstruction and selected pivot points for: (a) the $TwinDielTM$ target; (b) the $FoamDielintTM$ target; and (c) the $FoamTwinDielTM$ target; (d)–(f) real parts of the retrieved contrast profiles; (g)–(i) imaginary parts of the retrieved contrast profiles.

TABLE I
DETAILS OF THE INVERSION PROCEDURE FOR THE FRESNEL TARGETS

	TwinDiel	*FoamDielInt*	*FoamTwinDiel*
Frequency (GHz)	5	4	4
$\ell_D(\mathrm{cm})$	15	13	17
Data matrix	36×36	36×45	18×45
Ω_p, innermost points	$\lambda_b/5$	$\lambda_b/3$	$\lambda_b/2$
Ω_p, inner points	-	$\lambda_b/5$	$\lambda_b/4$
Ω_p, outermost points	$\lambda_b/10$	$\lambda_b/10$	$\lambda_b/8$

known to be critical for the LSM [27], [30], (i.e., a ring shaped scatterer).

To deal with such a case, the simulated data have been generated, under a full aspect configuration, by means of a full-wave method-of-moments-based forward solver and corrupted with a random gaussian noise with $\mathrm{SNR} = 15$ dB. Assuming, without loss of generality, that the filamentary currents used as transmitting and receiving probes are not in the close proximity of the imaging domain and that the background medium is vacuum, we have fixed the number of probes as $M = N \approx 8\ell_D/\lambda_b$, which, according to theoretical results, provides the nonredundant number of independent scattering experiments [22]. The resulting probes have been then evenly displaced in angle on a circumference of radius R.

The reconstruction's accuracy is appraised in terms of the mean square error (MSE)

$$MSE = \frac{\sum_{k=1}^{N_c} |\chi_k - \widetilde{\chi}_k|^2}{\sum_{k=1}^{N_c} |\chi_k|^2} \tag{14}$$

where N_c is the number of cells of the domain under investigation, χ_k and $\widetilde{\chi}_k$ the value of the actual contrast profile and of the reconstructed one in the kth cell, respectively.

The considered lossy dielectric ring is shown in Fig. 2(a) and (b). The parameters for this example are $\epsilon = 2.5$, $\sigma = 0.025$, $N_c = 64 \times 64$, $M = N = 21$, $R = 3.3\lambda_b$, the Tikhonov regularization parameter is equal to 8.3×10^{-5}. As expected, due to the multiple connection of the support and the circular symmetry of the contrast profile, the LSM fails in retrieving the actual shape, but can only provide an image of the target's convex hull, as indeed shown in Fig. 2(c). As a consequence, many of the selected pivot points do not lie within the actual target support. With respect to these points, we have set the radius of Ω_p, see Fig. 2(d)–(f), equal to $\lambda_b/2$, $\lambda_b/3$, and $\lambda_b/6$, respectively, and run the proposed regularized CSI scheme. It is interesting

Authorized licensed use limited to: UNIVERSIDADE FEDERAL DE MINAS GERAIS. Downloaded on May 28,2024 at 12:59:07 UTC from IEEE Xplore. Restrictions apply.

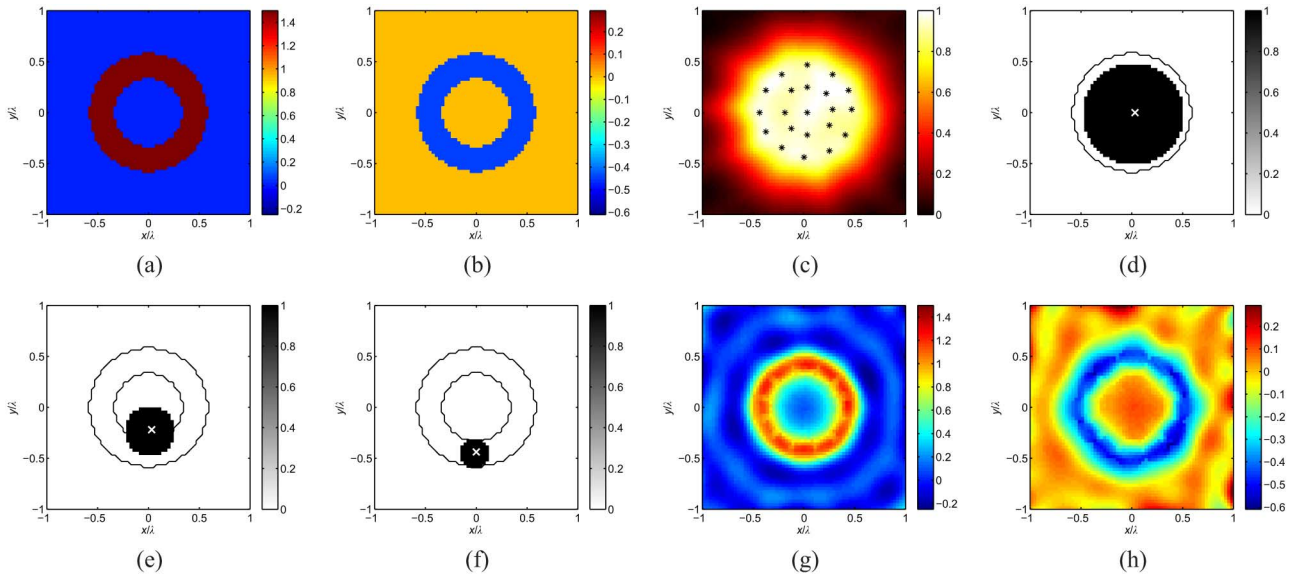

Fig. 2. Numerical example showing the capability of the proposed method of achieving successful results even when the estimated supports address a selection of pivot points lying outside of the actual support of the scatterer. (a) Real part and (b) imaginary part of the contrast profile; (c) LSM image, with the selected pivot points superimposed on it; (d) visual sketch of the circular region Ω_p for the innermost pivot point, a contour plot of the actual scatterer support is also depicted for visualization purposes; (e) same as (d), but for the inner pivots; (f) same as (d), but for the outermost pivot points; (g) real part and (h) imaginary part of the retrieved contrast.

to note that the final achieved result correctly guesses both the actual target's shape and its permittivity [see Figs. 2(g)–(h)] and corresponds to an MSE of 21%.

Such a result is only in apparent contradiction with the map in Fig. 2(c). In fact, it has to be stressed that, differently from the standard theory of LSM [where (8) is used to appraise the shape], in our case (8) is just used to enforce a circular symmetry of the contrast source. As a consequence (differently from the approach in [18] and [17]), in the present case the pivot points do not need to belong to the actual scatterer support. Rather, it is sufficient that virtual experiments are able to enforce some circularly symmetric contrast source around each one of the selected pivot points.

VII. Conclusion

In inverse scattering problems, the knowledge of internal fields (or contrast sources) plays a key role. In fact, the exact knowledge of these quantities would allow to consider a linear problem (rather than a nonlinear one) with obvious beneficial effects. On this line of reasoning, aimed to exploit information about contrast sources, we have presented in this paper a way to enforce a given structure to the contrast sources, and take advantage from such a knowledge. In fact, suitably designed virtual experiments allow to deal with circularly symmetric contrast sources, and one can easily take profit from such a circumstance by a simple modification of the usual CSI method. The effectiveness of the approach, which does not enforce any expected property of the contrast function, has been assessed against experimental data. Moreover, different from other contributions based on the recently introduced virtual experiments framework, the approach is also able to deal with nonsimply connected object.

The paradigm underlying this contribution offers a different, possibly complementary, point of view to improve the inversion, as compared to more usual regularization methods that act on the contrast function, and opens the way to new methods to tackle the inverse scattering problem. In fact, work is in progress to test performances of the technique in conjunction with regularization technique acting on the contrast function. Further improvements of the achievable results and reconstruction capabilities are indeed expected, similar to what has been recently observed when exploiting SOM in conjunction with MR [19]. Also, the extension of the whole framework and of the approach to the 2-D and three-dimensional (3-D) vectorial cases is currently under development.

Acknowledgment

The authors thank Dr. A. Litman and Dr. J.-M. Jeffrin from Institute Fresnel of Marseille, France for providing the $FoamDielIntTM$ inhomogeneous target dataset.

Appendix

We analytically derive the expression for the gradient and the line search parameter for the functional $\Phi(\mathcal{W}^{(1)}, \ldots, \mathcal{W}^{(P)})$, defined in (12), within a conjugate gradient scheme following the approach in [4].

To compute the gradient of Φ with respect to the generic contrast source $\mathcal{W}^{(p)}$, let us first recall that, by definition

$$\triangle\Phi_{\mathcal{W}^{(p)}} = \left\langle \nabla\Phi_{\mathcal{W}^{(p)}}, \triangle\mathcal{W}^{(p)} \right\rangle \tag{A.1}$$

wherein $\triangle\Phi_{\mathcal{W}^{(p)}}$ is the variation of Φ due to an increment of $\triangle\mathcal{W}^{(p)}$.

Authorized licensed use limited to: UNIVERSIDADE FEDERAL DE MINAS GERAIS. Downloaded on May 28,2024 at 12:59:07 UTC from IEEE Xplore. Restrictions apply.

Then from (12), it follows that

$$\triangle\Phi_{\mathcal{W}^{(p)}} = \left\{\left\langle \frac{\partial \mathcal{W}^{(p)}}{\partial \phi_p}, \frac{\partial \triangle \mathcal{W}^{(p)}}{\partial \phi_p} \right\rangle\right\} + \text{c.c.} \tag{A.2}$$

where $\langle \cdot, \cdot \rangle$ denotes usual scalar product, and c.c. stands for conjugate of the first addendum. Taking into account the properties of the involved differential operator [38], (A.2) can be rewritten as

$$\triangle\Phi_{\mathcal{W}^{(p)}} = \left\{\left\langle -\frac{\partial^2 \mathcal{W}^{(p)}}{\partial \phi_p^2}, \triangle \mathcal{W}^{(p)} \right\rangle\right\} + \text{c.c.} \tag{A.3}$$

and therefore

$$\nabla\Phi_{\mathcal{W}^{(p)}} = 2\left(-\frac{\partial^2 \mathcal{W}^{(p)}}{\partial \phi_p^2}\right). \tag{A.4}$$

To obtain the line search parameter, let us consider the behavior of functional (12) along an arbitrary line whose direction is given by $W^{(p)} + \lambda \triangle \mathcal{W}^{(p)}$ so that

$$\Phi[\mathcal{W}^{(p)} + \lambda \triangle \mathcal{W}^{(p)}] = \sum_{p=1}^{P} \left\{\left\langle \frac{\partial \mathcal{W}^{(p)}}{\partial \phi_p} + \lambda \frac{\partial \triangle \mathcal{W}^{(p)}}{\partial \phi_p}, \frac{\partial \mathcal{W}^{(p)}}{\partial \phi_p} + \lambda \frac{\partial \triangle \mathcal{W}^{(p)}}{\partial \phi_p} \right\rangle\right\}. \tag{A.5}$$

Due to the nature of the involved operator, (A.5) can be rewritten as a second degree algebraic polynomial, i.e.,

$$f(\lambda) = c_2 \lambda^2 + c_1 \lambda + c_0 \tag{A.6}$$

where

$$c_2 = \sum_{p=1}^{P} \left\| \frac{\partial \triangle \mathcal{W}^{(p)}}{\partial \phi_p} \right\|^2 \tag{A.7}$$

$$c_1 = 2\text{Re} \sum_{p=1}^{P} \left\{\left\langle \frac{\partial \mathcal{W}^{(p)}}{\partial \phi_p}, \frac{\partial \triangle \mathcal{W}^{(p)}}{\partial \phi_p} \right\rangle\right\} \tag{A.8}$$

$$c_0 = \sum_{p=1}^{P} \left\| \frac{\partial \mathcal{W}^{(p)}}{\partial \phi_p} \right\|^2. \tag{A.9}$$

Note that both in (A.4) and (A.7)–(A.9) the circular neighborhood Ω_p as defined in (12) acts to take into account the localized nature of the regularizing penalty term.

REFERENCES

[1] D. Colton and R. Kress, *Inverse Acoustic and Electromagnetic Scattering Theory*. Berlin, Germany: Springer-Verlag, 1992.

[2] R. E. Kleinman and P. M. van den Berg, "An extended modified gradient technique for profile inversion," *J. Geophys. Res.*, vol. 28, no. 2, pp. 877–884, 1993.

[3] P. M. van den Berg and R. E. Kleinman, "A contrast source inversion method," *Inv. Prob.*, vol. 13, no. 6, pp. 1607–1620, 1997.

[4] T. Isernia, V. Pascazio, and R. Pierri, "A nonlinear estimation method in tomographic imaging," *IEEE Trans. Geosci. Remote Sens.*, vol. 35, no. 4, pp. 910–923, Jul. 1997.

[5] T. Isernia, L. Crocco, and M. D' Urso, "New tools and series for forward and inverse scattering problems in lossy media," *IEEE Trans. Geosci. Remote Sens. Lett.*, vol. 1, no. 4, pp. 327–331, Oct. 2004.

[6] X. Chen, "Subspace-based optimization method for solving inverse-scattering problems," *IEEE Trans. Geosci. Remote Sens.*, vol. 48, no. 1, pp. 42–49, Jan. 2010.

[7] T. Isernia, V. Pascazio, and R. Pierri, "On the local minima in a tomographic imaging technique," *IEEE Trans. Geosci. Remote Sens.*, vol. 39, no. 7, pp. 1596–1607, Jul. 2001.

[8] M. Bertero, "Linear inverse and ill-posed problems," in *Advances in Electronics and Electron Physics*. New York, NY, USA: Academic, 1989.

[9] P. M. van den Berg, A. Abubakar, and J. T. Fokkema, "Multiplicative regularization for contrast profile inversion," *Radio Sci.*, vol. 38, no. 2, pp. 23.1–23.10, 2003.

[10] P. M. van den Berg and R. E. Kleinman, "A total variation enhanced modified gradient algorithm for profile reconstruction," *Inverse Prob.*, vol. 11, no. 3, pp. L5–L10, 1995.

[11] I. Catapano *et al.*, "On quantitative microwave tomography of female breast," *Prog. Electromagn. Res.*, vol. 97, pp. 75–93, 2009.

[12] R. Scapaticci, I. Catapano, and L. Crocco, "Wavelet-based adaptive multiresolution inversion for quantitative microwave imaging of breast tissues," *IEEE Trans. Antennas Propag.*, vol. 60, no. 8, pp. 3717–3726, Aug. 2012.

[13] M. Li, O. Semerci, and A. Abubakar, "A contrast source inversion method in the wavelet domain," *Inverse Prob.*, vol. 29, no. 2, p. 025015, 2013.

[14] L. Crocco, I. Catapano, L. Di Donato, and T. Isernia, "The linear sampling method as a way for quantitative inverse scattering," *IEEE Trans. Antennas Propag.*, vol. 4, no. 60, pp. 1844–1853, Apr. 2012.

[15] L. Di Donato, M. Bevacqua, T. Isernia, I. Catapano, and L. Crocco, "Improved quantitative microwave tomography by exploiting the physical meaning of the linear sampling method," in *Proc. IEEE 5th Eur. Conf. Antennas Propag. (EuCAP)*, Apr. 11–15, 2011, pp. 3828–3831.

[16] L. Crocco, I. Catapano, L. Di Donato, and T. Isernia, "Enhancing the factorization method relying on its physical meaning," in *Proc. IEEE 7th Eur. Conf. Antennas Propag. (EuCAP)*, Apr. 8–12, 2013, pp. 70–71.

[17] M. Bevacqua, L. Di Donato, L. Crocco, and T. Isernia, "Conditioning inverse scattering problems by means of suitably designed synthetic experiments," in *Proc. 8th Eur. Conf. Antennas Propag. (EUCAP)*, 2014, pp. 1336–1339.

[18] M. Bevacqua, L. Crocco, L. Di Donato, and T. Isernia, "An algebraic solution method for nonlinear inverse scattering," *IEEE Trans. Antennas Propag.*, vol. 63, no. 2, pp. 601–610, Feb. 2015.

[19] K. Xu, Y. Zhong, R. Song, X. Chen, and L. Ran, "Multiplicative-regularized FFT twofold subspace-based optimization method for inverse scattering problems," *IEEE Trans. Geosci. Remote Sens.*, vol. 53, no. 2, pp. 841–850, Feb. 2015.

[20] K. Belkebir and M. Saillard, "Guest editors' introduction," *Inverse Prob.*, vol. 17, pp. 1565–1571, 2001.

[21] K. Belkebir and M. Saillard, "Guest editors' introduction," *Inverse Prob.*, vol. 21, no. 6, pp. S1–S3, 2004.

[22] O. M. Bucci and T. Isernia, "Electromagnetic inverse scattering: Retrievable information and measurement strategies," *Radio Sci.*, vol. 32, pp. 2123–2138, 1997.

[23] O. M. Bucci, L. Crocco, and T. Isernia, "Improving the reconstruction capabilities in inverse scattering problems by exploitation of close-proximity setups," *J. Opt. Soc. Amer. A*, vol. 16, pp. 1788–1798, 1999.

[24] O. M. Bucci and G. Franceschetti, "On the spatial bandwidth of the scattered fields," *IEEE Trans. Antennas Propag.*, vol. 35, no. 12, pp. 1445–1455, Dec. 1987.

[25] O. M. Bucci and G. Franceschetti, "On the degrees of freedom of scattered fields," *IEEE Trans. Antennas Propag.*, vol. 37, no. 7, pp. 918–926, Jul. 1989.

[26] F. Cakoni and D. Colton, *Qualitative Methods in Inverse Scattering Theory*. Berlin, Germany: Springer-Verlag, 2006.

[27] I. Catapano, L. Crocco, and T. Isernia, "On simple methods for shape reconstruction of unknown scatterers," *IEEE Trans. Antennas Propag.*, vol. 55, no. 5, pp. 1431–1436, May 2007.

[28] I. Catapano, L. Crocco, M. D' Urso, and T. Isernia, "3D microwave imaging via preliminary support reconstruction: Testing on the Fresnel 2008 database," *Inverse Prob.*, vol. 25, no. 2, pp. 1–23, 2009.

[29] L. Crocco, L. Di Donato, D. A. M. Iero, and T. Isernia, "An adaptive method to focusing in unknown scenario," *Prog. Electromagn. Res.*, vol. 130, pp. 563–579, 2012.

[30] L. Crocco, L. Di Donato, I. Catapano, and T. Isernia, "An improved simple method for imaging the shape of complex targets," *IEEE Trans. Antennas Propag.*, vol. 61, no. 2, pp. 843–851, Feb. 2013.

[31] D. Colton, H. Haddar, and M. Piana, "The linear sampling method in inverse electromagnetic scattering theory," *Inverse Prob.*, vol. 19, pp. 105–137, 2003.

Authorized licensed use limited to: UNIVERSIDADE FEDERAL DE MINAS GERAIS. Downloaded on May 28,2024 at 12:59:07 UTC from IEEE Xplore. Restrictions apply.

[32] C. Gilmore, P. Mojabi, and J. LoVetri, "Comparison of an enhanced distorted born iterative method and the multiplicative-regularized contrast source inversion method," *IEEE Trans. Antennas Propag.*, vol. 57, no. 8, pp. 2341–2351, Aug. 2009.
[33] A. Abubakar, P. M. van den Berg, and T. M. Habashy, "Application of the multiplicative regularized contrast source inversion method on TM and TE polarized experimental fresnel data," *Inverse Prob.*, vol. 21, no. 6, pp. S5–S13, 2005.
[34] L. Crocco and T. Isernia, "Inverse scattering with real data: detecting and imaging homogeneous dielectric objects," *Inverse Prob.*, vol. 17, no. 6, p. 1573, 2001.
[35] L. Crocco, M. D'Urso, and T. Isernia, "Testing the contrast source extended Born inversion method against real data: The TM case," *Inverse Prob.*, vol. 21, p. S33, 2005.
[36] J. LoVetri, P. Mojabi, and L. Shafai, "A multiplicative regularized gauss-inversion inversion for shape and location reconstruction," *IEEE Trans. Antennas Propag.*, vol. 59, no. 12, pp. 4790–4802, Dec. 2011.
[37] I. Catapano and L. Crocco, "An imaging method for concealed targets," *IEEE Trans. Geosci. Remote Sens.*, vol. 47, no. 5, pp. 1301–1309, May 2009.
[38] L. V. Kantorovich and G. P. Alkilov, *Functional Analysis*. Moscow, Russia: Nauka, 1977.

Loreto Di Donato received the M.S. Laurea degree in biomedical engineering from the University of Naples Federico II, Naples, Italy, in 2008, and the Ph.D. degree in information engineering from Mediterranea University of Reggio di Calabria, Reggio Calabria, Italy, in 2012.

In 2009, he joined the Institute for Electromagnetic Sensing of the Environment, National Research Council of Italy (IREA-CNR), Naples, Italy, as a Research Assistant. Since 2013, he has been with the Department of Electric, Electronics, and Computer Sciences, University of Catania, Catania, Italy, as an Assistant Professor in electromagnetic fields. His research activities include inverse scattering problems, with a particular interest in biomedical and subsurface noninvasive diagnostics, as well as synthesis problems.

Dr. Di Donato was a Young Scientist Awardee at the XXX URSI General Assembly in 2011.

Martina Teresa Bevacqua was born in Reggio Calabria, Italy, in 1988. She received the M.S. Laurea degree (*summa cum laude*) in electronic engineering from Mediterranea University of Reggio Calabria, Reggio Calabria, Italy, in 2012. Currently, she is working toward the Ph.D. degree at Mediterranea University of Reggio di Calabria.

Her research activities include electromagnetic inverse scattering problems with particular interest in biomedical and subsurface noninvasive diagnostics.

Dr. Bevacqua was the recipient of the "G. Barzilai" Award from the Italian Electromagnetics Society in 2014.

Lorenzo Crocco (SM'10) was born in Naples, Italy, in 1971. He received the Laurea degree (*summa cum laude*) in electronic engineering and the Ph.D. degree in applied electromagnetics from the University of Naples Federico II, Naples, Italy, in 1995 and 2000, respectively.

Since 2001, he has been a Research Scientist with the Institute for Electromagnetic Sensing of the Environment, National Research Council of Italy (IREA-CNR), Naples, Italy. From 2009 to 2011, he was an Adjunct Professor with Mediterranea University of Reggio Calabria, Reggio Calabria, Italy, where he currently is a Member of the Board of Ph.D. advisors. He has published more than 60 papers on peer reviewed international journals, given keynote talks at international conferences, and lead or actively contributed to Italian and European research projects. His research interests include electromagnetic scattering problems, imaging methods for noninvasive diagnostics, through the wall radar and ground-penetrating radar, as well as microwave biomedical imaging, and therapeutic uses of electromagnetic fields.

Dr. Crocco has served as a Guest Editor for international scientific journals. Currently, he is a Member of the Management Committee of COST Action TD1301 on microwave medical imaging. He is a Fellow of The Electromagnetics Academy (TEA). He was the recipient of the "Barzilai" Award for Young Scientists from the Italian Electromagnetic Society in 2004 and Young Scientist Awardee at the XXVIII URSI General Assembly in 2005. In 2009, he was awarded as one of the top one-hundred under 40 scientists of CNR.

Tommaso Isernia (M'93) received the Laurea degree (*summa cum laude*) and the Ph.D. degree in electronic engineering from the University of Naples Federico II, Naples, Italy.

From 1992 to 1998, he was an Assistant Professor and from 1998 to 2003, an Associate Professor with the University of Naples Federico II. Currently, he is a Full Professor in Electromagnetic Fields with the Mediterranea University of Reggio Calabria, Reggio Calabria, Italy, wherein he also serves as a Member of the Board of Administrators and as "Presidente dei Corsi di Studio in Ingegneria dell' Informazione." His research interests include inverse problems in electromagnetics with particular emphasis on phase retrieval, inverse scattering, and antenna synthesis problems. Recently, he is also engaged in field synthesis problems for biomedical imaging and therapeutic applications.

Dr. Isernia was the recipient of the "G. Barzilai" Award from the Italian Electromagnetics Society in 1994.

Authorized licensed use limited to: UNIVERSIDADE FEDERAL DE MINAS GERAIS. Downloaded on May 28,2024 at 12:59:07 UTC from IEEE Xplore. Restrictions apply.